U.S. DEPARTMENT OF THE INTERIOR

U.S. GEOLOGICAL SURVEY

Mineralogical and geochemical analyses of three paleosols from the Merced Formation, near San Francisco, California

by

Gretchen Luepke[1]

Open-File Report 91-104

---

[1] U.S. Geological Survey, Menlo Park, California

1991

Table of Contents Page

List of figures

List of Tables

MINERALOGICAL AND GEOCHEMICAL ANALYSES OF THREE PALEOSOLS FROM THE MERCED FORMATION, NEAR SAN FRANCISCO, CALIFORNIA

Gretchen Luepke

Abstract

Variations in the mineralogy and geochemistry among three paleosols examined in the Merced Formation may reflect varying changes in importance of sediment source area more than changes related strictly to soil-forming conditions. Percentage of opaque minerals is the major factor influencing the geochemical makeup of a sample regardless of the sample's stratigraphic position.

Introduction

Paleosols occur at several horizons in the upper part (upper 300 m stratigraphically) of the Merced Formation in the cliffs south of San Francisco, California (Fig. 1). This part of the formation has been determined to be of Pleistocene age (Clifton and others, 1988). Paleosols occur within dune and alluvial facies (Clifton and Hunter, 1987). No paleosols in the Merced Formation have previously been studied mineralogically or chemically. The purpose of this paper is to make a preliminary examination of three selected paleosols to see if any differences would be found between them and their presumed parent material (represented by underlying and overlying relatively unweathered sediments), that can be detected through the use of mineralogical or geochemical analyses, and to determine if this method of inquiry would warrant further study.

Description

The Merced Formation is a sequence of repetitive cycles representing shelf to subaerial sedimentation. Paleosols within the Merced Formation are readily recognized by sharp upper contacts, erosional resistance (due to the presence of iron oxides and clay), an overall lack of stratification, and gradational bases. Root structures and/or subsoil lamellae may be present. The generalized stratigraphic section in Figure 1 shows the stratigraphic location of the paleosols examined in this study.

Paleosol 1 is in the upper part of unit U_3 (dune facies). Paleosols 2 and 3 are part of unit R_3 (a paleosol unit with interbedded backshore and alluvial sand). The asterisk in Figure 1 shows the location of Sample 15, taken in unit V_4, 1-1.5 m below a soil in unit V_5 (alluvial facies). This sample served as a comparison between dune and alluvial facies in this study.

The stratigraphic order of the samples is depicted in Figure 2. Paleosols 1 (samples 10-14) and 2 (samples 3-7) were sampled in detail, including samples in the well-stratified sediments above the paleosol surfaces and stratified sediments below the paleosols. Paleosol 3, a grayish yellow green unit (5GY 7/2; Goddard, 1948) below Paleosol 2, was sampled only at its top and in the stratified layer above it (samples 8 and 9). The colors of all remaining samples fell within the yellow-brown hues (5YR-10YR; Goddard, 1948); such colors are characteristic of B and C soil horizons (Birkeland, 1984, p. 13).

Methods

Each sample was washed and air-dried. A split (average weight, 26 g) was made from each sample for separation in tetrabromoethane (S.G.=2.96). Heavy minerals were separated and counted using standard techniques. After the split for heavy-mineral separation had been made, the remaining part of each sample was analyzed for clay minerals--smectite, illite, and chlorite plus kaolinite--after the method of Hein and others. (1976). In brief, the procedure is as follows: Carbonate was removed with Morgan's solution (sodium acetate plus glacial acetic acid diluted with distilled water), and organic matter removed with 30 percent sodium peroxide. The clay-size fraction (<0.002 mm) was isolated by centrifugation, and each sample Mg-saturated and glycolated. An X-ray diffractogram was made after glycolation. Clay-mineral percentages were calculated from peak areas

The light minerals were examined using a staining method modified form Force and others (1982, p. 4): 1-5 g of microsplit light-mineral fraction was placed in a small plastic beaker and etched in 52 percent HF for about 10 sec. It was next rinsed three times, and then immersed for at least 15 min in a concentrated solution of sodium cobaltinitrite. After rinsing off the cobaltinitrite, the samples were examined, using a binocular microscope, to visually estimate the percentage of potash feldspar (hereafter referred to as K-spar), which had been stained bright yellow by the cobaltinitrite (Hayes and Klugman, 1959). Plagioclase retained an opaque white coating, while quartz remained uncoated, using this method.

Splits of both the heavy- and light-mineral fractions of each sample were analyzed for major and minor elements. Geochemical analyses were performed at the USGS analytical labs in Denver, Colorado, using optical spectroscopy and a modified induced-coupled semi-quantitative process (Lichte and others, 1987). The samples were digested into a sodium peroxide sinter in a zirconium crucible (Borsier and Garcia, 1983). For this reason, the following elements could not be tested for: sodium in the major elements, and germanium, tin, tungsten, and zirconium in the minor elements.

Results

Nonopaque heavy minerals identified in the samples include orthopyroxene (mostly hypersthene), clinopyroxene (mostly augite), hornblende (green, blue-green, brown, and basaltic), tremolite/ actinolite, epidote group (epidote, clinozoisite, and zoisite), glaucophane, apatite, zircon, rutile, sphene, and tourmaline. Opaque minerals were not determined in detail, but magnetite was detected in all samples. Ilmenite and chromite are probably also present. Aggregates are commonly iron-stained grains composed of more than one mineral that cannot be precisely identified. In the light-mineral fraction, quartz, plagioclase, alkali feldspar (K-spar), and rock fragments were identified. Percentages of heavy and light minerals, with averages and standard deviations, for each sample are given in Table 1. Geochemical analyses of the major and minor elements found within the heavy-mineral fraction are given in Table 2, within the light fraction in Table 3.

Among the heavy minerals, there is little obvious variation among the nonopaque minerals. Percentages of opaque minerals show no consistent patterns. Among the light minerals, plagioclase and quartz together account for over 75 percent of all light minerals. From visual estimation, a slight depletion of K-spar occurs at the tops of the three paleosols, when compared to the overlying samples. Potassium percentages in the light-mineral fractions (Table 3) generally support these observations, although the analyses show no significant variability.

Only three samples contained clay minerals. Samples 3 and 8 both lie at the top of their respective paleosols in dune facies; the clay mineral in both is 100% smectite. Sample 15, taken within an alluvial unit, contained a clay mineral analysis of 55.6% chlorite plus kaolinite, 23.2% illite, and 21.2% smectite.

Discussion

Q-mode factor analyses were performed on the nonopaque heavy-mineral and geochemical data. The heavy-mineral data is divided into the following two factors by the analysis:

Factor 1: orthopyroxene, clinopyroxene, garnet, zircon, rutile

Factor 2: hornblende, epidote, sphene, glaucophane, -rutile

Figure 3a shows the plot of the factors for the heavy-mineral data. These factors represent the two previously identified source areas for the Merced sedimentary basin (Hall, 1965). These sources are the Sierra Nevada and Great Valley sediments delivered via the Sacramento-San Joaquin river system (key mineral, hypersthene, the most common orthopyroxene), and rocks from the local Franciscan Complex (key mineral, glaucophane). The samples as plotted show a continuum rather than discrete clusters. The random gradation of heavy-mineral composition among the samples indicates the variation in importance of the source area at the time of deposition rather than particular distinctions among the paleosols.

Two factors were also found among the geochemistry of major and minor elements (of both the heavy-mineral and light-mineral fractions) and may be separated as follows:

Factor	Heavy minerals	Light minerals
1	Al, Ca, K, Mg -Ce, Co, Cr, Cu, La, Mn, Nb, Ni V, Y, Yb, Zn	Ca, Fe, Mg, P B, -Ba, Co, Li, Mn, Ni -Sr, V, Zn
2	Fe, Ti, B, Ba, Ce, Ga Sc, Sr, Th	K, -Ti, Ba, -Cr, La, Sr, -Zn

Figures 3b-e show the plots of the factors for the geochemical data. Samples 3, 8, and 10 were taken at the uppermost surface of their respective paleosols. Sample 8, representing the greenish paleosol, shows up as distinctively different from Sample 10 in all four geochemical categories. Sample 3, however, is similar to Sample 8 in major and minor elements of heavy minerals, and similar to Sample 10 in major and minor elements of light minerals. Therefore, no one factor can differentiate the uppermost surfaces.

As a second comparison, Samples 7, 9, and 14 were taken above the paleosol surfaces. The light minerals of these three samples show similar geochemistries in both the major and minor elements. The geochemistry of the heavy minerals appears to reflect the pattern seen in the percentages of heavy minerals. These groupings show that samples for an individual paleosol cannot readily be separated based on stratigraphic position. On the contrary, samples from an individual paleosol tend to cluster together, indicating little geochemical distinctiveness related to weathering during soil development.

In the geochemical groupings among the heavy minerals, the samples may be roughly clustered as follows: Factor-1-dominant (Samples 7, 10, 11, 12, 13, and 15); and Factor-2-dominant (Samples 3, 4, 5, 6, 8, 9, and 14). When the percentages of opaque heavy minerals among these samples are compared in a Student's T statistical test, the Factor-1-dominant samples show a mean opaque mineral percentage of 21.5 (± 6.4), while the Factor-2-dominant samples show 13.3 (± 5.4). These values are statistically dissimilar at a 95 percent confidence level, or the probability that they are alike is $P = 0.034$. Therefore, the geochemistry of the heavy minerals within a samples seems to depend primarily on the concentration of opaque minerals within that sample.

Sample 8 is distinctive because of its greenish color. Colors in this range indicate reducing conditions (Birkeland, 1984, p. 13). All other samples in this study showed the yellow-brown and red colors indicative of oxidizing conditions. The exact nature of the reducing conditions cannot be determined at this time.

Sample 15, the only one taken in an alluvial facies, stands out from the rest of the samples based on mineralogy and geochemistry of heavy minerals. It is also the only sample to show the presence of clay minerals other than smectite. Detailed sampling of specific alluvial paleosols in the Merced Formation would be needed to determine if mineralogical and geochemical patterns were comparable to those seen among dune paleosols.

Conclusions

Routine mineralogical and geochemical analyses do not readily distinguish among the paleosols of the Merced Formation that were examined in this study. Clay minerals, lacking in the paleosols of the dune facies, may (based on data from a single sample in this study) be important constituents in an alluvial facies. The paleosols studied in this report may represent only the preserved C horizons, with the mineralogy reflecting sorting more strongly than weathering processes. Alternatively, both B and C horizons may be present, but the degree of soil development was not great enough to produce distinct mineralogical and geochemical changes in the sediments.

References

Birkeland, P.W., 1984, Soils and geomorphology: Oxford University Press, New York. 372 p.

Borsier, M. and Garcia, M., 1983, Analyse automatique d'échantillons géologiques par plasma ICP: Spectrochimica Acta, v. 38B, no. 1-2, p. 123-127.

Bortugno, E.J., McJunkin, R.D., and Wagner, D.L., in press, Geologic map of the San Francisco-San Jose Quadrangle: California division of Mines and Geology, scale 1:250,000.

Clifton, H.E. and Hunter, R.E., 1987, The Merced Formation and related beds--a mile-thick succession of late Cenozoic coastal and shelf deposits in the sea cliffs off San Francisco, California: Geological Society of America Centennial Field Guide, Cordilleran Section, v. 1, p 257-262.

Clifton, H.E., Hunter, R.E., and Gardner, J.V., 1988, Analysis of eustatic, tectonic, and sedimentologic influences on transgressive and regressive cycles in the upper Cenozoic Merced Formation, San Francisco, California, *in* Kleinspehn, K.L., and Paola, C., eds., New perspectives in basin analysis: New York, Springer-Verlag Inc., p. 109-128.

Force, E.R., Grosz, A.E., Loferski, P.J., and Maybin, A.H., 1982, Aeroradioactivity maps in heavy-mineral exploration--Charleston, South Carolina, area: U.S. Geological Survey Professional Paper 1218, 19 p.

Goddard, E.N.(chairman),1948, Rock-Color Chart: prepared by the Rock-Color Chart Committee, National Research Council, Washington, D.C.

Hall, N.T., 1965, Petrology of the type Merced Group, San Francisco peninsula, California: Berkeley, University of California M.A. thesis, 126 p.

Hayes, J.R.and Klugman, M.A., 1959, Feldspar staining methods: Journal of Sedimentary Petrology, v. 29, n. 2, p. 227-232.

Hein, J.R., Scholl, D.W., and Gutmacher, C.E., 1976, Neogene clay minerals of the far NW Pacific and southern Bering Sea, *in* Bailey, S.W., ed., International Clay Conference, Mexico City, 1975, Proceedings: Willmette, Illinois, Applied Publishing Ltd., p. 71-80.

Lichte, F.E., Golighhtly, D.W., and Lamothe, P.J., 1987, Inductively coupled plasma-atomic emission spectrometry: in Baedecker, P.A., eds., Methods of geochemical analysis, U.S. Geological Survey Bulletin 1770, Chapter B, 10 p.

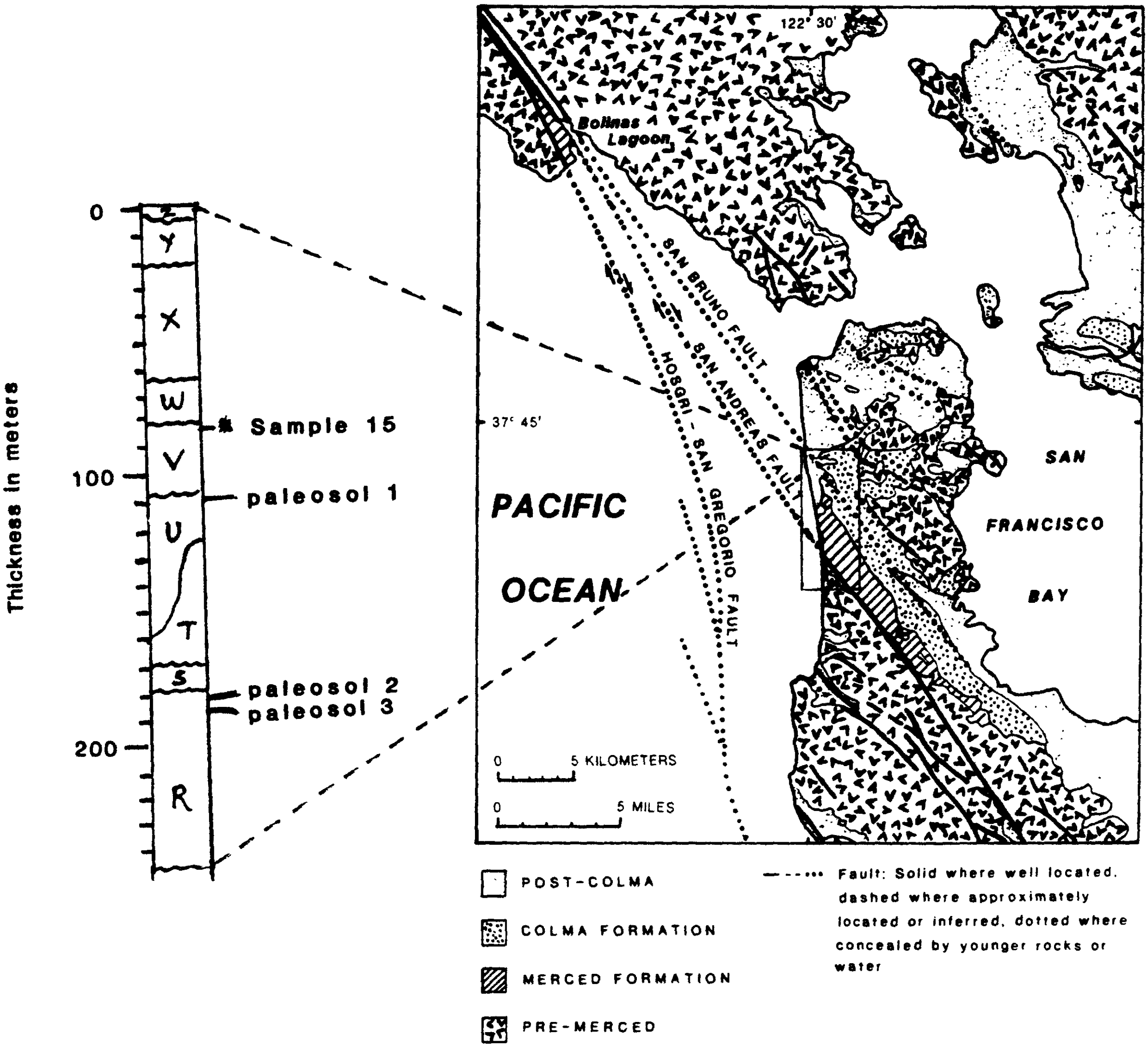

Figure 1. Index map showing location of study area (in box) of the Merced Formation. Generalized stratigraphic section shows location of paleosols described in this report. Map from Clifton and others, 1988; geology generalized from Bortugno and others, in press. Letters in stratigraphic column denote sequences of Clifton and others, 1988.

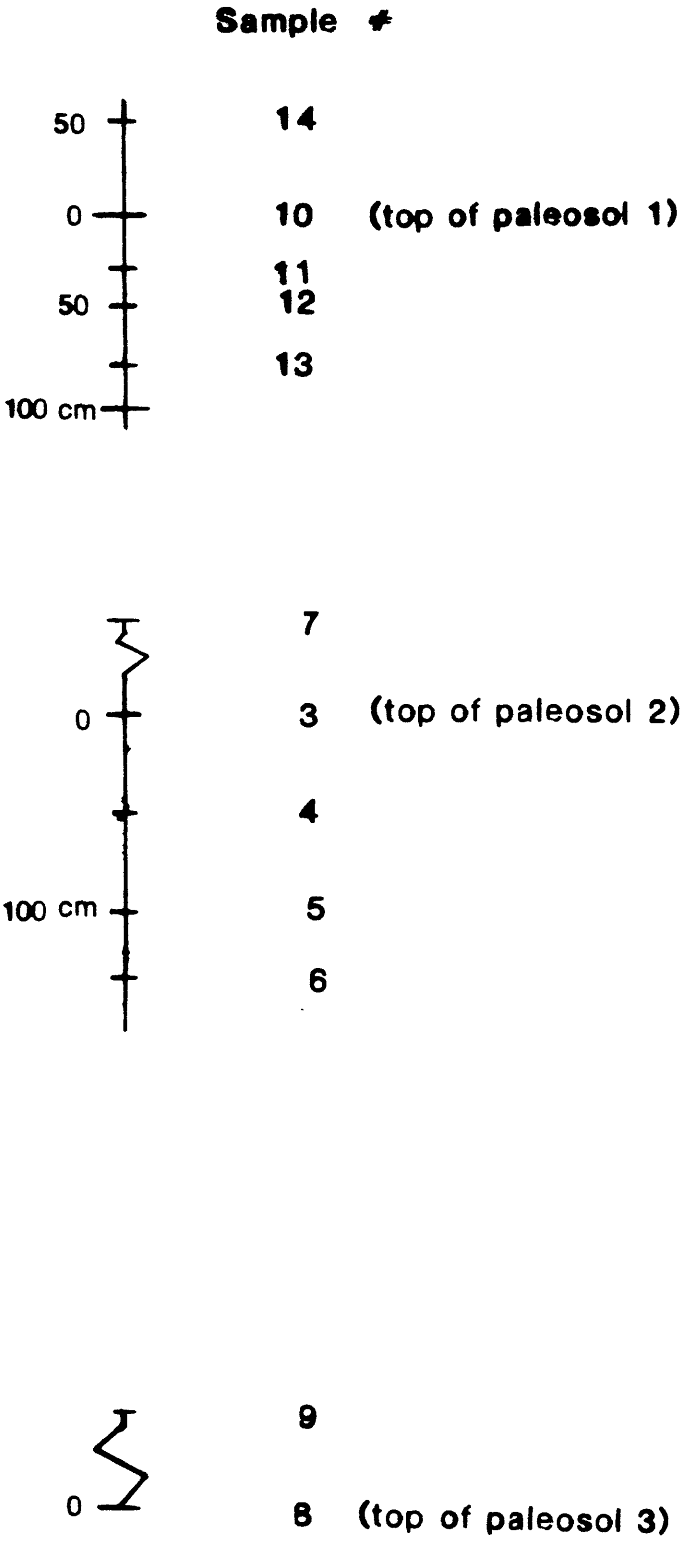

Figure 2. Relative stratigraphic position of samples in paleosols described in this report. For position of Sample 15, see Figure 1.

Figure 3.

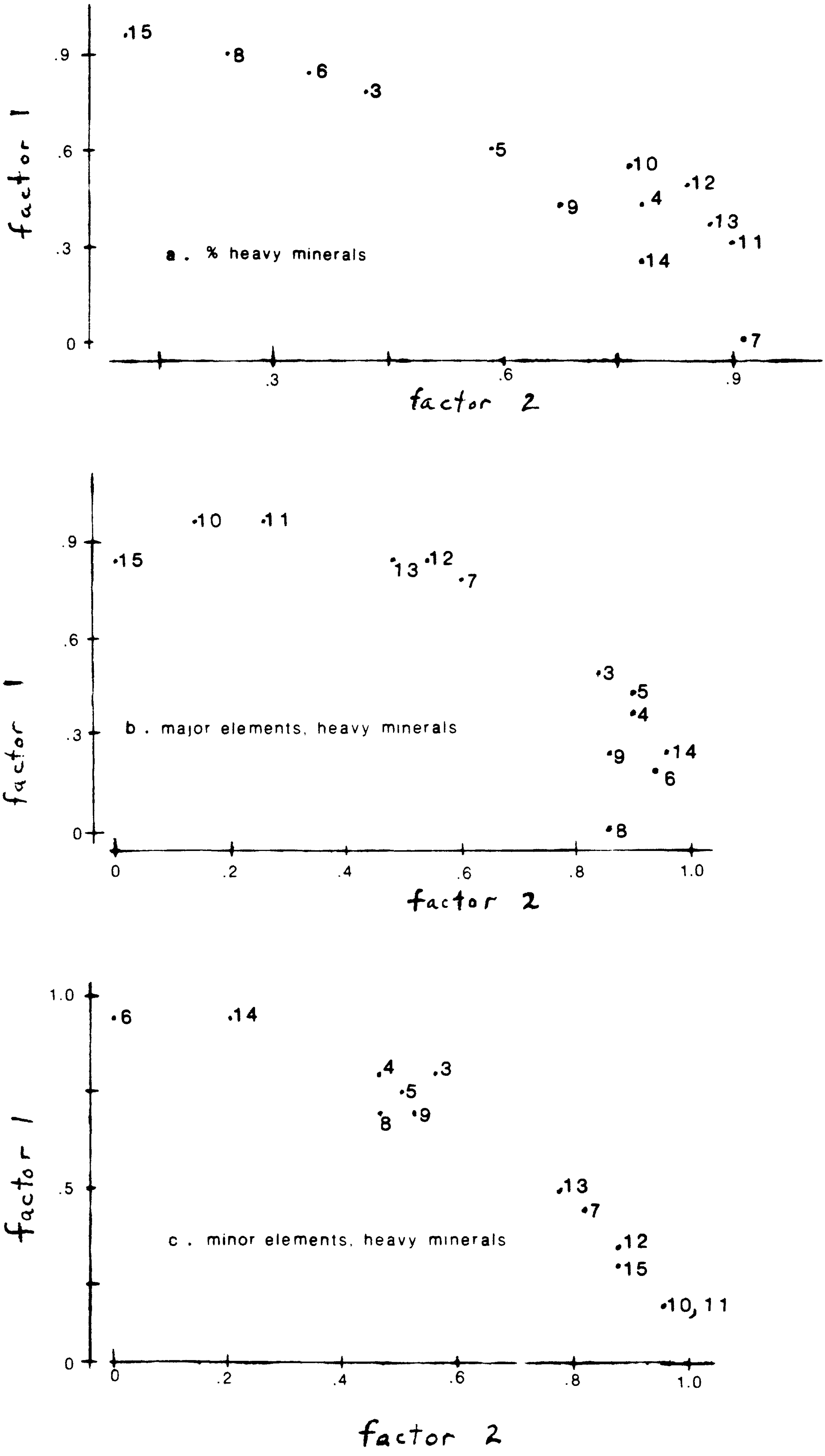
a . % heavy minerals
factor 1
factor 2
.9
.6
.3
0
.3
.6
.9
15
8
6
3
5
10
12
4
9
13
11
14
7
b . major elements, heavy minerals
factor 1
factor 2
.9
.6
.3
0
0
.2
.4
.6
.8
1.0
10
11
15
13
12
7
3
5
4
9
14
6
8
c . minor elements, heavy minerals
factor 1
factor 2
1.0
.5
0
0
.2
.4
.6
.8
1.0
6
14
4
3
5
8
9
13
7
12
15
10, 11

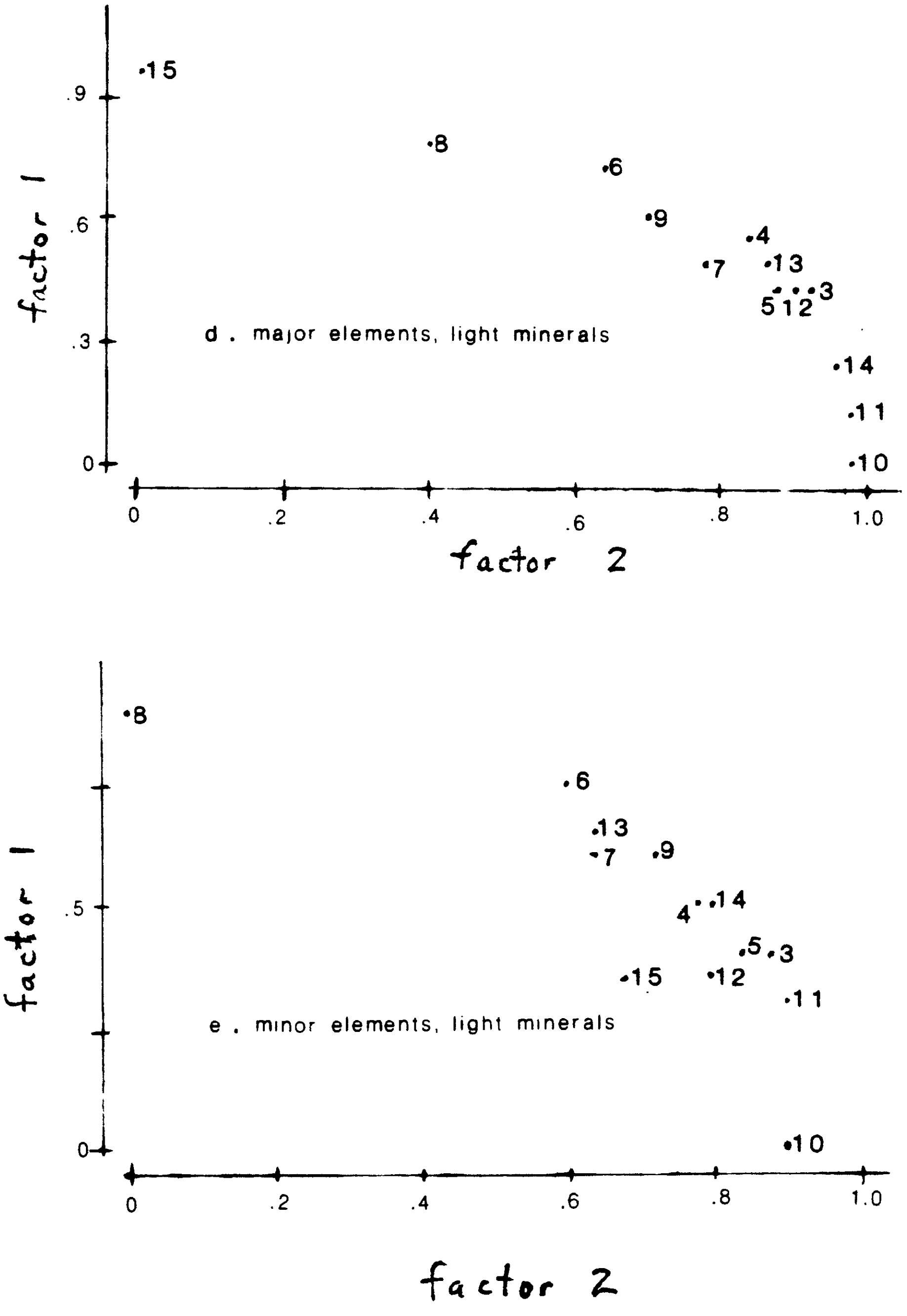

Figure 3. Plots of Q-mode factor analyses from Merced Formation paleosols. a) percent nonopaque heavy minerals; b) major elements in heavy minerals; c) minor elements in heavy minerals; d) major elements in light minerals; e) minor elements in light minerals.

Table 1. Heavy and light minerals in paleosols of the Merced Formation

Mineral		Paleosol			1		Paleosol			2		Paleosol	3	Average	Standard deviation
	#15	#14	#10	#11	#12	#13	#7	#3	#4	#5	#6	#9	#8		
Opaques	26.7	7.1	20.0	28.9	11.0	19.3	23.3	17.8	19.6	17.7	8.0	14.8	8.3	17.1	7.0
Aggregates	6.8	23.0	31.1	21.1	34.0	41.0	35.9	23.9	26.6	29.9	23.0	21.4	8.5	25.1	9.8
Nonopaques	66.5	69.9	48.9	50.0	55.0	39.7	40.8	58.3	53.8	52.4	69.0	63.8	83.2	57.8	12.4
Orthopyroxene	16.3	26.9	22.5	24.0	21.9	20.0	25.4	13.1	14.8	13.4	17.7	28.8	13.2	19.8	5.5
Clinopyroxene	6.9	18.6	16.7	16.4	14.6	19.2	16.8	11.2	19.6	18.5	13.8	17.3	10.5	15.4	3.8
Hornblende	46.7	31.8	30.8	32.4	36.1	35.2	24.0	35.4	36.6	36.6	45.3	32.1	42.9	35.8	6.2
Basaltic Hornblende	2.4	1.9	1.8	2.2	2.3	2.0	3.1	3.7	1.1	2.8	1.8	2.9	6.6	2.7	1.4
Tremolite/ Actinolite	2.4	1.5	0.7	—	0.8	—	0.7	2.2	1.4	0.8	—	0.3	2.7	1.0	0.9
Glaucophane	0.4	1.1	*	—	*	*	—	—	—	—	*	—	0.3	—	—
Epidote group	21.9	13.3	23.2	20.0	19.6	19.2	17.2	28.7	19.9	23.6	18.1	13.6	20.1	19.9	4.1
Sphene	1.6	1.1	0.7	1.1	1.5	0.8	0.7	1.5	0.7	0.8	2.1	1.5	0.9	1.1	0.4
Garnet	0.4	1.1	1.4	1.8	1.5	0.8	1.7	1.1	1.1	0.4	0.4	0.4	0.6	1.0	0.5
Apatite	*	*	*	—	*	*	0.3	0.4	—	—	*	0.7	*	—	—
Zircon	0.8	1.5	1.8	1.4	0.8	2.4	8.6	1.1	3.9	2.8	0.7	1.1	0.3	2.1	2.2
Rutile	—	0.4	—	0.4	*	*	0.7	*	—	—	*	—	—	—	—
Tourmaline	—	*	—	—	—	—	—	—	*	—	—	0.4	—	—	—
Unknowns	—	0.8	0.4	0.4	0.8	0.4	0.7	1.5	0.7	0.4	—	0.8	1.8	0.7	0.5
K-feldspar	10	10	5	10	15	10	15	10	10	1	10	10	5	9	3.8
Plagioclase	10	15	15	15	15	15	15	15	15	15	15	15	15	20	2.0
Quartz	77	68	73	68	60	68	65	65	65	74	65	64	72	68	4.6
Rock frags.	3	7	7	7	10	7	5	10	10	10	10	5	3	7	2.6

*=mineral seen in sample but not encountered during the grain count.

Table 2. Geochemical analyses of heavy minerals in paleosols of the Merced Formation.

Element		Paleosol 1					Paleosol 2					Paleosol 3		Average	Standard Deviation	Detection Limits
	#15	#14	#10	#11	#12	#13	#7	#3	#4	#5	#6	#9	#8			
Al (pct)	4.5	5.2	4.0	4.2	4.6	4.4	4.6	4.8	5.1	4.9	5.6	4.2	4.8	4.7	0.4	0.02
Ca	6.7	9.0	6.7	7.0	7.8	7.7	7.9	8.2	8.7	8.5	9.1	8.2	8.6	8.0	0.8	0.02
Fe	18.0	11.0	17.0	17.0	15.0	16.0	15.0	13.0	13.0	13.0	11.0	12.0	10.0	13.9	2.6	0.02
K	0.2	0.3	0.2	0.2	0.2	0.2	0.2	0.3	0.3	0.3	0.4	0.3	0.3	0.3	0.1	0.20
Mg	5.3	6.4	4.9	5.2	5.7	5.6	5.6	5.4	5.6	5.8	5.7	7.5	7.1	5.8	0.7	0.02
P	0.03	0.07	0.07	0.07	0.07	0.06	0.06	0.06	0.06	0.06	0.07	0.05	0.03	0.06	0.01	0.02
Ti	2.8	1.6	3.0	2.9	2.5	2.4	2.2	1.9	1.7	1.8	1.5	1.6	2.0	2.1	0.5	0.02
Ag (ppm)	L	L	L	L	L	L	L	L	L	L	L	L	L			8
As	L	L	L	L	L	L	L	L	L	L	L	L	L			40
Au	L	L	L	L	L	L	L	L	L	L	L	L	L			30
B	70	80	50	50	70	60	70	70	60	70	80	60	60	65	10	16
Ba	51	64	58	58	63	61	56	63	65	64	74	65	56	61	6	4
Be	L	L	L	L	L	L	L	L	L	L	L	L	L			4
Bi	L	L	L	L	L	L	L	L	L	L	L	L	L			40
Cd	L	L	L	L	L	L	L	L	L	L	L	L	L			8
Ce	L	80	L	L	L	40	L	60	80	70	80	90	90	45	39	20
Co	72	55	73	72	65	67	65	57	57	57	47	60	55	62	8	4
Cr	7800	3700	9600	8700	7400	7000	8800	6000	5400	5400	2700	3000	3700	61	23	4
Cu	9	6	29	18	29	7	11	8	7	19	6	34	5	14	10	4
Eu	L	L	L	L	L	L	L	L	L	L	L	L	L			8
Ga	20	20	20	L	L	30	20	20	20	L	30	20	L	15	11	16
Ho	L	L	L	L	L	L	L	L	L	L	L	L	L			16
La	100	75	96	110	100	110	84	84	100	87	68	90	89	92	12	8
Li	L	9	L	L	L	L	L	L	L	L	10	10	L			8
Mn	3300	2700	3300	3200	3100	3100	2900	2600	2500	2600	2400	2700	2800	2860	310	16
Mo	L	L	9	L	L	L	L	L	L	L	L	L	L			8
Nb	30	L	30	30	30	30	20	20	20	20	L	20	30	21	11	16
Nd	100	110	90	100	80	120	80	100	90	70	90	100	100	95	13	16
Ni	120	120	130	140	140	130	130	130	130	130	120	140	120	129	8	8
Pb	L	L	L	L	L	L	L	L	L	L	L	L	L			16
Sc	50	65	53	55	57	57	54	55	56	57	66	61	62	57	5	8
Sr	270	290	210	230	250	240	280	290	310	300	310	240	300	271	33	8
Ta	L	L	L	L	L	L	L	L	L	L	L	L	L			160
Th	30	40	40	40	30	60	30	40	30	40	30	50	60	40	11	16
U	L	L	L	L	L	L	L	L	L	L	L	L	L			400
V	650	390	650	650	570	570	530	490	460	460	390	390	360	505	107	8
Y	87	69	77	70	71	88	74	65	62	62	67	70	85	73	9	8
Yb	11	8	10	9	9	11	9	8	7	8	8	8	10	9	1	4
Zn	230	130	230	220	200	190	180	150	140	140	130	150	150	172	38	8

L=limits of detection

Table 3. Geochemical analysis of light minerals of the Merced Formation.

Element		Paleosol 1					Paleosol 2					Paleosol 3		Average	Standard Deviation
	#15	#14	#10	#11	#12	#13	#7	#3	#4	#5	#6	#9	#8		
Al (pct)	4.8	5.3	5.5	5.4	5.1	4.9	4.8	5.3	5.3	5.2	5.3	6.3	5.7	5.3	0.4
Ca	1.3	1.7	2.1	1.9	1.6	1.6	1.5	1.7	1.7	1.6	1.4	1.9	1.7	1.7	0.2
Fe	1.2	1.8	2.8	2.5	1.9	1.6	1.6	2.0	1.9	1.9	1.7	2.0	1.3	1.9	0.4
K	1.2	1.0	0.9	1.0	1.1	1.1	1.2	1.2	1.3	1.2	1.3	1.4	1.3	1.2	0.1
Mg	0.32	0.82	1.10	0.92	0.71	0.64	0.64	0.88	0.85	0.80	0.66	0.86	0.52	0.75	0.20
P	L	0.02	0.03	0.03	0.02	0.02	0.03	0.03	0.03	0.03	0.02	0.02	L	0.02	0.01
Ti	0.12	0.17	0.28	0.23	0.15	0.14	0.14	0.18	0.15	0.15	0.13	0.17	0.14	0.16	0.04
Ag (ppm)	L	L	L	L	L	L	L	L	L	L	L	L	L		
As	L	L	L	L	L	L	L	L	L	L	L	L	L		
Au	L	L	L	L	L	L	L	L	L	L	L	L	L		
B	20	20	30	20	20	20	20	30	30	20	20	30	20	23	5
Ba	470	410	390	430	450	450	470	470	500	470	500	540	510	466	41
Be	L	L	L	L	L	L	L	L	L	L	L	L	L		
Bi	L	L	L	L	L	L	L	L	L	L	L	L	L		
Cd	L	L	L	L	L	L	L	L	L	L	L	L	L		
Ce	L	L	L	L	L	L	L	L	L	L	L	L	L		
Co	15	11	15	13	9	9	9	12	10	11	10	11	7	11	2
Cr	120	110	320	280	140	110	130	210	130	150	92	130	130	158	69
Cu	5	9	L	7	L	L	19	12	15	7	5	9	L	7	6
Eu	L	L	L	L	L	L	L	L	L	L	L	L	L		
Ga	L	L	L	L	L	L	L	L	20	L	20	L	L		
Ho	L	L	L	L	L	L	L	L	L	L	L	L	L		
La	9	12	11	11	L	11	10	12	12	L	16	12	8	9	5
Li	11	11	10	9	8	10	10	12	13	9	15	16	L	10	4
Mn	600	310	400	360	310	250	240	290	260	260	210	270	140	300	111
Mo	L	L	L	L	L	L	L	L	L	L	L	L	L		
Nb	L	L	L	L	L	L	L	L	L	L	L	L	L		
Nd	20	L	L	L	L	20	L	30	30	L	L	L	L		
Ni	24	48	55	53	42	35	48	63	62	54	52	47	19	46	13
Pb	L	L	L	L	L	L	L	L	L	L	L	L	L		
Sc	L	L	10	L	L	L	L	L	L	10	L	L	L		
Sr	220	250	260	250	240	230	240	250	250	250	260	310	300	255	25
Ta	L	L	L	L	L	L	L	L	L	L	L	L	L		
Th	20	L	L	L	L	20	L	L	30	L	L	L	L		
U	L	L	L	L	L	L	L	L	L	L	L	L	L		
V	38	47	78	65	46	42	44	59	53	54	42	68	47	52	12
Y	L	L	L	L	L	L	L	L	L	L	L	L	L		
Yb	L	L	L	L	L	L	L	L	L	L	L	L	L		
Zn	25	29	41	36	28	25	25	32	30	30	26	36	24	30	5

L=Limits of detection. Detection limits listed in Table 2.